European Journal of Mechanics A/Solids 30 (2011) 517–524

Contents lists available at ScienceDirect

European Journal of Mechanics A/Solids

journal homepage: www.elsevier.com/locate/ejmsol

A size-dependent Kirchhoff micro-plate model based on strain gradient elasticity theory

Binglei Wang [a,b], Shenjie Zhou [a,*], Junfeng Zhao [a], Xi Chen [b,c,d,**]

[a] School of Mechanical Engineering, Shandong University, Jinan, Shandong 250061, China
[b] Department of Earth and Environmental Engineering, Columbia University, New York, NY 10027, USA
[c] Department of Civil & Environmental Engineering, Hanyang University, Seoul 133-791, South Korea
[d] School of Aerospace, Xi'an Jiaotong University, Xi'an 710049, China

ARTICLE INFO

Article history:
Received 25 May 2010
Accepted 1 April 2011
Available online 8 April 2011

Keywords:
Size effect
Strain gradient elasticity
Micro-plate

ABSTRACT

A size-dependent Kirchhoff micro-plate model is developed based on the strain gradient elasticity theory. The model contains three material length scale parameters, which may effectively capture the size effect. The model can also degenerate into the modified couple stress plate model or the classical plate model, if two or all of the material length scale parameters are taken to be zero. The static bending, instability and free vibration problems of a rectangular micro-plate with all edges simple supported are carried out to illustrate the applicability of the present size-dependent model. The results are compared with the reduced models. The present model can predict prominent size-dependent normalized stiffness, buckling load, and natural frequency with the reduction of structural size, especially when the plate thickness is on the same order of the material length scale parameter.

1. Introduction

Recent technological developments have opened up promising research opportunities and engineering priorities in micro-plate based micromechanics (Batra et al., 2007), in which the plate thickness is typically on the order of microns or sub-microns. The size-dependent behavior of micron-scale structures has been proven experimentally in metals (Nix, 1989; Fleck et al., 1994; Poole et al., 1996), geomaterials and brittle materials (Vardoulakis et al., 1998), polymers (Lam and Chong, 1999; Lam et al., 2003; McFarland and Colton, 2005) and polysilicon (Chasiotis and Knauss, 2003). The classical theory of linear elasticity is characterized by the local character of stress without any internal (material) length scale, which is inadequate for predicting the mechanical behavior of small material structures, whose behavior is characterized by non-local stresses and the existence of an internal length scale.

Higher-order continuum theories have recently raised the interest of many scientists (Batra, 1987; Fleck et al., 1994; Vardoulakis et al., 1998; Lam et al., 2003; Papargyri-Beskou et al., 2003, 2010; Reddy, 2007a; Papargyri-Beskou and Beskos, 2008; Kong et al., 2009; Wang et al., 2010), in which strain gradient or non-local terms are involved and additional material length scale parameters are consequently introduced to complement the classical material constants. A review of the high order elasticity theories can be found in the works of (Vardoulakis and Sulem, 1995; Exadaktylos and Vardoulakis, 2001; Papargyri-Beskou and Beskos, 2008).

Based on the aforementioned higher-order continuum theories, several micro-plate models have been developed by many researchers based on micropolar theory (Ariman, 1968a,b); the simplest version of the simplified form-II theory of strain gradient linear elasticity due to Mindlin (1964) (Papargyri-Beskou and Beskos, 2009; Vavva et al., 2009; Papargyri-Beskou et al., 2010); gradient elastic theory (Lazopoulos, 2004, 2009); and couple stress theory (Hoffman, 1964; Ellis and Smith, 1967; Tsiatas, 2009). Ariman (1968a,b) studied the circular micropolar plate and discussed some problems in the model. Lazopoulos (2004) established a strain gradient elasticity theory of plates, based on the gradient elasticity theory proposed by Altan and Aifantis (1997) which can be traced back to Mindlin (1965). The theory is applied to the study of the buckling behavior of a long rectangular plate under uniaxial compression and small lateral load, supported on a rigid plane foundation. Recently, Lazopoulos (2009) studied the bending of strain gradient elastic thin plates, adopting a simple version of Mindlin's linear theory of elasticity with microstructure, in which

* Corresponding author.
** Corresponding author. Department of Earth and Environmental Engineering, Columbia University, New York, NY 10027, USA.
E-mail addresses: zhousj@sdu.edu.cn (S. Zhou), xichen@columbia.edu (X. Chen).

0997-7538/$ – see front matter © 2011 Elsevier Masson SAS. All rights reserved.
doi:10.1016/j.euromechsol.2011.04.001

the intrinsic bulk length g and the directional surface energy length l_k are introduced to characterize the strain gradient in addition to the classical Lame constants. Tsiatas (2009) presented a micro Kirchhoff plate model for the static analysis of isotropic micro-plates with arbitrary shape based on the simplified couple stress theory of Yang et al. (2002) containing only one material length scale parameter, rendering a relatively simple formulation of the size-dependent plate model. Vavva et al. (2009) studied the velocity dispersion curves of guided modes propagating in an isotropic micro-plate based on the simplified Mindlin (1964, 1965) form-II gradient elastic theory. Very recently, Papargyri-Beskou et al. (2010) studied the gradient elastic flexural Kirchhoff plates under static loading via variational method, and derived the exact boundary condition for any plate form and showed validated the effectiveness of the approximate boundary conditions proposed by Papargyri-Beskou and Beskos (2008).

Shu and Fleck (1998) pointed out that the couple stress theory (Fleck and Hutchinson, 1993), which is a general form of the modified couple stress theory (Yang et al., 2002) used by Tsiatas (2009) to predict the size effect of micro-plate, usually under-predicts the size effect because the couple stress theory only employs the rotation gradient and neglects the other gradients (e.g. stretch gradient). Therefore, to more effectively account for the size effect, a general strain gradient theory, incorporating not only the rotation gradient but also stretch gradient or other gradients, should be introduced.

Among the higher-order continuum theories, the strain gradient elasticity theory proposed by Lam et al. (2003) was successfully applied to predict the size-dependent properties for small scale structures. Three material length scale parameters are introduced to characterize the dilatation gradient tensor, the deviatoric stretch gradient tensor, and the symmetric rotation gradient tensor, respectively. Through work conjugation, the higher-order stress tensors are related to the higher-order deformation metrics. The theory has been used to analyze the static and dynamic problems of micro scale Bernoulli–Euler beam (Kong et al., 2009) and Timoshenko beam (Wang et al., 2010). Moreover, it should be noted that strain gradient elasticity theory of Lam et al. (2003) can degenerate into the modified couple stress theory of Yang et al. (2002) by setting two of the three material length scale parameters to zero; thus, the strain gradient elasticity theory (Lam et al., 2003) may be regarded as a much wider extension of the modified couple stress theory (Yang et al., 2002).

The objective of this work is to develop a size-dependent Kirchhoff plate model based on the strain gradient elasticity theory (Lam et al., 2003). In Section 2, the governing equation of the size-dependent Kirchhoff micro-plate is derived. In subsequent Sections 3–5, the size-dependence of the normalized stiffness, critical load, and natural frequency for the simple supported plate are described and discussed. Conclusions are summarized in Section 6.

2. Governing equations of size-dependent flexural plate

Based on the higher-order stress theory (Mindlin, 1965), Lam et al. (2003) proposed the strain gradient elasticity theory, in which a new additional equilibrium equation governing the behavior of higher-order stresses, the equilibrium of moments of couples, is introduced in addition to the classical equilibrium equations of forces and moments. There are three material length scale parameters for isotropic linear elastic materials.

According to the theory, the total deformation energy density is a function of the symmetric strain tensor, the dilatation gradient vector, the deviatoric stretch gradient tensor and the symmetric rotation gradient tensor. The strain energy U in a deformed isotropic linear elastic material occupying region Ψ (with a volume element V) is given by

$$U = \frac{1}{2}\int_V \bar{u}\,\mathrm{d}\Psi = \frac{1}{2}\iiint_V \bar{u}\,\mathrm{d}x\mathrm{d}y\mathrm{d}z \tag{1}$$

in which $\bar{u}$ is the strain energy density, defined by

$$\bar{u} = \sigma_{ij}\varepsilon_{ij} + p_i\gamma_i + \tau_{ijk}^{(1)}\eta_{ijk}^{(1)} + m_{ij}^s\chi_{ij}^s \tag{2}$$

For the indices (subscripts) throughout this paper, the repeated indices denote summation from 1 to 3. And the deformation measures, i.e., the strain tensor, ε_{ij}, the dilatation gradient tensor, γ_i, the deviatoric stretch gradient tensor, $\eta_{ijk}^{(1)}$, and the symmetric rotation gradient tensor, χ_{ij}^s, are defined by

$$\varepsilon_{ij} = \frac{1}{2}\left(\partial_j u_i + \partial_i u_j\right) \tag{3}$$

$$\eta_{ijk}^{(1)} = \eta_{ijk}^s - \frac{1}{5}\left(\delta_{ij}\eta_{mmk}^s + \delta_{jk}\eta_{mmi}^s + \delta_{ki}\eta_{mmj}^s\right) \tag{4}$$

$$\gamma_i = \partial_i\varepsilon_{mm} \tag{5}$$

and

$$\chi_{ij}^s = \frac{1}{4}\left(e_{ipq}\partial_p\varepsilon_{qj} + e_{jpq}\partial_p\varepsilon_{qi}\right) \tag{6}$$

respectively. Here, ∂_i is the differential operator, u_i is the displacement vector, ε_{mm} is the dilatation strain, and η_{ijk}^s is the symmetric part of the second order displacement gradient tensor defined by

$$\eta_{ijk}^s = \frac{1}{3}\left(u_{i,jk} + u_{j,ki} + u_{k,ij}\right) \tag{7}$$

where δ_{ij} and e_{ijk} are the Knocker delta and permutation tensor, respectively.

The stress measures (detailed physical interpretation of the higher-order stresses can be found in Lam et al. (2003)) include the classical stress tensor, σ_{ij}, and the higher-order stresses, p_i, $\tau_{ijk}^{(1)}$, and m_{ij}^s, which are the work-conjugate to the deformation measures, are given by the following constitutive relations,

$$\sigma_{ij} = k\delta_{ij}\varepsilon_{mm} + 2\mu\varepsilon'_{ij} \tag{8}$$

$$p_i = 2\mu l_0^2\gamma_i \tag{9}$$

$$\tau_{ijk}^{(1)} = 2\mu l_1^2\eta_{ijk}^{(1)} \tag{10}$$

$$m_{ij}^s = 2\mu l_2^2\chi_{ij}^s \tag{11}$$

where ε_{ij}' is the deviatoric strain defined as

$$\varepsilon'_{ij} = \varepsilon_{ij} - \frac{1}{3}\varepsilon_{mm}\delta_{ij} \tag{12}$$

k and μ are the bulk and shear modulus, respectively. l_0, l_1 and l_2 are the additional independent material length scale parameters associated with the dilatation gradients, deviatoric stretch gradients, and symmetric rotation gradients, respectively.

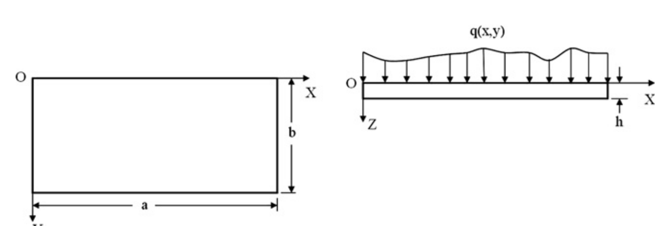

Fig. 1. Schematic of a micro-plate with distributed load.

Consider an initially flat thin rectangular elastic plate of thickness h, subjected to a static transverse load $q(x,y)$ distributed in the x–y plane as depicted in Fig. 1. The length and width of the plate are a and b. The plate is made by homogeneous linearly elastic material. According to Kirchhoff's plate theory, the displacement field can be described as

$$\begin{aligned} u_x(x,y,z) &= -z\frac{\partial w(x,y)}{\partial x} \\ u_y(x,y,z) &= -z\frac{\partial w(x,y)}{\partial y} \\ u_z(x,y,z) &= w(x,y) \end{aligned} \tag{13}$$

where $u_i(x,y,z)$ $(i=x,y,z)$are displacement components along X, Y, Z directions.

Substituting Eq. (13) into Eq.(3), the nonzero components of the strain tensor are written as

$$\begin{aligned} \varepsilon_{xx} &= -z\frac{\partial^2 w}{\partial x^2} \\ \varepsilon_{yy} &= -z\frac{\partial^2 w}{\partial y^2} \\ \varepsilon_{xy} &= -z\frac{\partial^2 w}{\partial x\partial y} \end{aligned} \tag{14}$$

where ε_{ij} $(i=x,y,z)$ are strain components.

The other three gradient tensors γ_i, $\eta^{(1)}_{ijk}$, χ^s_{ij} are deduced by substituting Eqs. (13) and (14) into Eqs. (4)–(6), and the results are presented in Appendix. Subsequently, the work-conjugate stress tensors σ_{ij}, p_i, $\tau^{(1)}_{ijk}$, and m^s_{ij} are calculated by substituting these strain tensors into Eqs. (8)–(11), respectively. Finally, when the strain and stress tensors are substituted into Eqs. (1) and (2), we obtain the strain energy density $\overline{u}$ by taking somewhat lengthy but straightforward manipulations:

$$\begin{aligned} \overline{u} = {} & \left(c_1+c_2z^2\right)\left(\left(\frac{\partial^2 w}{\partial x^2}\right)^2+\left(\frac{\partial^2 w}{\partial y^2}\right)^2\right)+\left(c_3+c_4z^2\right)\left(\frac{\partial^2 w}{\partial x^2}\frac{\partial^2 w}{\partial y^2}\right) \\ & +\left(c_5+c_6z^2\right)\left(\frac{\partial^2 w}{\partial x\partial y}\right)^2+c_7z^2\left(\left(\frac{\partial^3 w}{\partial x^3}\right)^2+\left(\frac{\partial^3 w}{\partial y^3}\right)^2\right) \\ & +c_8z^2\left(\left(\frac{\partial^3 w}{\partial x\partial y^2}\right)^2+\left(\frac{\partial^3 w}{\partial x^2\partial y}\right)^2\right) \\ & +c_9z^2\left(\frac{\partial^3 w}{\partial x^3}\frac{\partial^3 w}{\partial x\partial y^2}+\frac{\partial^3 w}{\partial y^3}\frac{\partial^3 w}{\partial x^2\partial y}\right) \end{aligned} \tag{15}$$

in which

$$\begin{aligned} c_1 &= 2\mu l_0^2+\frac{8}{15}\mu l_1^2+\mu l_2^2; \quad c_2 = \left(k+\frac{4}{3}\mu\right) \\ c_3 &= 4\mu l_0^2-\frac{4}{15}\mu l_1^2-2\mu l_2^2; \quad c_4 = \left(2k-\frac{4}{3}\mu\right) \\ c_5 &= \frac{4}{3}\mu l_1^2+4\mu l_2^2; \quad c_6 = 4\mu \\ c_7 &= 2\mu l_0^2+\frac{4}{5}\mu l_1^2; \quad c_8 = 2\mu l_0^2+\frac{24}{5}\mu l_1^2 \\ c_9 &= 4\mu l_0^2-\frac{12}{5}\mu l_1^2 \end{aligned} \tag{16}$$

Assuming the following integral relations,

$$\begin{aligned} &\iiint_V z^2\,\mathrm{d}x\mathrm{d}y\mathrm{d}z = I\iint_A \mathrm{d}x\mathrm{d}y \quad I = \int_{-h/2}^{h/2} z^2\,\mathrm{d}z = \frac{h^3}{12} \\ &\iiint_V \mathrm{d}x\mathrm{d}y\mathrm{d}z = h\iint_A \mathrm{d}x\mathrm{d}y \end{aligned} \tag{17}$$

The variation of strain energy can be written as

$$\begin{aligned} \delta U &= \iiint_V \delta\overline{u}\,\mathrm{d}x\mathrm{d}y\mathrm{d}z = \iint_S \delta F\,\mathrm{d}x\mathrm{d}y \\ &= \iint_S\left(\frac{\partial F}{\partial w_{xx}}\delta w_{xx}+\frac{\partial F}{\partial w_{yy}}\delta w_{yy}+\frac{\partial F}{\partial w_{xy}}\delta w_{xy}+\frac{\partial F}{\partial w_{xxx}}\delta w_{xxx}\right. \\ &\quad\left.+\frac{\partial F}{\partial w_{yyy}}\delta w_{yyy}+\frac{\partial F}{\partial w_{xyy}}\delta w_{xyy}+\frac{\partial F}{\partial w_{xxy}}\delta w_{xxy}\right)\mathrm{d}x\mathrm{d}y \end{aligned} \tag{18}$$

in which

$$\begin{aligned} F = {} & (c_1h+c_2I)\left(\left(\frac{\partial^2 w}{\partial x^2}\right)^2+\left(\frac{\partial^2 w}{\partial y^2}\right)^2\right) \\ & +(c_3h+c_4I)\left(\frac{\partial^2 w}{\partial x^2}\frac{\partial^2 w}{\partial y^2}\right)+(c_5h+c_6I)\left(\frac{\partial^2 w}{\partial x\partial y}\right)^2 \\ & +c_7I\left(\left(\frac{\partial^3 w}{\partial x^3}\right)^2+\left(\frac{\partial^3 w}{\partial y^3}\right)^2\right)+c_8I\left(\left(\frac{\partial^3 w}{\partial x\partial y^2}\right)^2+\left(\frac{\partial^3 w}{\partial x^2\partial y}\right)^2\right) \\ & +c_9I\left(\frac{\partial^3 w}{\partial x^3}\frac{\partial^3 w}{\partial x\partial y^2}+\frac{\partial^3 w}{\partial y^3}\frac{\partial^3 w}{\partial x^2\partial y}\right) \end{aligned} \tag{19}$$

and

$$\begin{aligned} & w_{xx}=\frac{\partial^2 w}{\partial x^2}, \quad w_{yy}=\frac{\partial^2 w}{\partial y^2}, \quad w_{xy}=\frac{\partial^2 w}{\partial x\partial y} \\ & w_{xxx}=\frac{\partial^3 w}{\partial x^3}, \quad w_{yyy}=\frac{\partial^3 w}{\partial y^3}, \quad w_{xxy}=\frac{\partial^3 w}{\partial x^2\partial y}, \quad w_{xyy}=\frac{\partial^3 w}{\partial x\partial y^2} \end{aligned} \tag{20}$$

By applying the rules of integration by parts, Eq. (18) is rewritten as

$$\begin{aligned} \delta U = {} & \iint\left(\frac{\partial^2}{\partial x^2}\left(\frac{\partial F}{\partial w_{xx}}\right)+\frac{\partial^2}{\partial y^2}\left(\frac{\partial F}{\partial w_{yy}}\right)+\frac{\partial^2}{\partial x\partial y}\left(\frac{\partial F}{\partial w_{xy}}\right)-\frac{\partial^3}{\partial x^3}\left(\frac{\partial F}{\partial w_{xxx}}\right)-\frac{\partial^3}{\partial y^3}\left(\frac{\partial F}{\partial w_{yyy}}\right)-\frac{\partial^3}{\partial x\partial y^2}\left(\frac{\partial F}{\partial w_{xyy}}\right)-\frac{\partial^3}{\partial x^2\partial y}\left(\frac{\partial F}{\partial w_{xxy}}\right)\right)\delta w\,\mathrm{d}x\mathrm{d}y \\ & +\int\left(\frac{\partial F}{\partial w_{yy}}\delta w_y\Big|_0^b-\frac{\partial}{\partial y}\left(\frac{\partial F}{\partial w_{yy}}\right)\delta w\Big|_0^b-\frac{\partial}{\partial x}\left(\frac{\partial F}{\partial w_{xy}}\right)\delta w\Big|_0^b+\frac{\partial F}{\partial w_{yyy}}\delta w_{yy}\Big|_0^b-\frac{\partial}{\partial y}\left(\frac{\partial F}{\partial w_{yyy}}\right)\delta w_y\Big|_0^b+\frac{\partial^2}{\partial y^2}\left(\frac{\partial F}{\partial w_{yyy}}\right)\delta w\Big|_0^b-\frac{\partial}{\partial x}\left(\frac{\partial F}{\partial w_{xyy}}\right)\delta w_y\Big|_0^b\right. \\ & \left.+\frac{\partial^2}{\partial x\partial y}\left(\frac{\partial F}{\partial w_{xyy}}\right)\delta w\Big|_0^b+\frac{\partial^2}{\partial x^2}\left(\frac{\partial F}{\partial w_{xxy}}\right)\delta w\Big|_0^b\right)\mathrm{d}x+\int\left(\frac{\partial F}{\partial w_{xx}}\delta w_x\Big|_0^a-\frac{\partial}{\partial x}\left(\frac{\partial F}{\partial w_{xx}}\right)\delta w\Big|_0^a+\frac{\partial}{\partial y}\left(\frac{\partial F}{\partial w_{xy}}\right)\delta w\Big|_0^a+\frac{\partial F}{\partial w_{xxx}}\delta w_{xx}\Big|_0^a-\frac{\partial}{\partial x}\left(\frac{\partial F}{\partial w_{xxx}}\right)\delta w_x\Big|_0^a\right. \\ & \left.+\frac{\partial^2}{\partial x^2}\left(\frac{\partial F}{\partial w_{xxx}}\right)\delta w\Big|_0^a+\frac{\partial^2}{\partial y^2}\left(\frac{\partial F}{\partial w_{xyy}}\right)\delta w\Big|_0^a-\frac{\partial}{\partial y}\left(\frac{\partial F}{\partial w_{xxy}}\right)\delta w_x\Big|_0^a+\frac{\partial^2}{\partial x\partial y}\left(\frac{\partial F}{\partial w_{xxy}}\right)\delta w\Big|_0^a\right)\mathrm{d}y \end{aligned} \tag{21}$$

The first variation of the work done by the external force, $q(x,y)$, takes the form

$$\delta W = \int_0^a \int_0^b q(x,y)\delta w(x,y)\,\mathrm{d}x\mathrm{d}y \tag{22}$$

Substituting Eqs. (21) and (22) into the following expression of principle of minimum potential energy,

$$\delta(U-W) = 0 \tag{23}$$

Due to the variational principle for arbitrary δw, the governing equation is finally obtained by taking somewhat lengthy but straightforward manipulations:

$$-p_1\nabla^6 w + p_2\nabla^4 w = q(x,y) \tag{24}$$

in which

$$\begin{aligned} p_1 &= I\mu\left(2l_0^2+\frac{4}{5}l_1^2\right)\\ p_2 &= \mu h\left(2l_0^2+\frac{8}{15}l_1^2+l_2^2\right)+\left(k+\frac{4}{3}\mu\right)I \end{aligned} \tag{25}$$

and

$$\begin{aligned} \nabla^6 w &= \frac{\partial^6 w}{\partial x^6}+3\frac{\partial^6 w}{\partial x^4\partial y^2}+3\frac{\partial^6 w}{\partial x^2\partial y^4}+\frac{\partial^6 w}{\partial y^6}\\ \nabla^4 w &= \frac{\partial^4 w}{\partial x^4}+2\frac{\partial^4 w}{\partial x^2\partial y^2}+\frac{\partial^4 w}{\partial y^4} \end{aligned} \tag{26}$$

The corresponding exact boundary conditions at the edges can also be obtained:

$$\begin{aligned} &B_{X1}(a,y)\delta w(a,y)-B_{X1}(0,y)\delta w(0,y) = 0\\ &B_{X2}(a,y)\delta w_x(a,y)-B_{X2}(0,y)\delta w_x(0,y) = 0\\ &B_{X3}(a,y)\delta w_{xx}(a,y)-B_{X3}(0,y)\delta w_{xx}(0,y) = 0\\ &B_{Y1}(x,b)\delta w(x,b)-B_{Y1}(x,0)\delta w(x,0) = 0\\ &B_{Y2}(x,b)\delta w_y(x,b)-B_{Y2}(x,0)\delta w_y(x,0) = 0\\ &B_{Y3}(x,b)\delta w_{yy}(x,b)-B_{Y3}(x,0)\delta w_{yy}(x,0) = 0 \end{aligned} \tag{27}$$

in which

$$\begin{aligned} B_{X1}(x,y) &= -2P_1\frac{\partial^3 w}{\partial x^3}-(P_2+2P_3)\frac{\partial^3 w}{\partial x\partial y^2}+2P_4\frac{\partial^5 w}{\partial x^5}+(2P_5+2P_6)\frac{\partial^5 w}{\partial x^3\partial y^2}+(2P_5+P_6)\frac{\partial^5 w}{\partial x\partial y^4}\\ B_{X2}(x,y) &= 2P_1\frac{\partial^2 w}{\partial x^2}+P_2\frac{\partial^2 w}{\partial y^2}-2P_4\frac{\partial^4 w}{\partial x^4}-(2P_5+P_6)\frac{\partial^4 w}{\partial x^2\partial y^2}-P_6\frac{\partial^4 w}{\partial y^4}\\ B_{X3}(x,y) &= 2P_4\frac{\partial^3 w}{\partial x^3}+P_6\frac{\partial^3 w}{\partial x\partial y^2}\\ B_{Y1}(x,y) &= -2P_1\frac{\partial^3 w}{\partial y^3}-(P_2+2P_3)\frac{\partial^3 w}{\partial x^2\partial y}+2P_4\frac{\partial^5 w}{\partial y^5}+(2P_5+2P_6)\frac{\partial^5 w}{\partial x^2\partial y^3}+(2P_5+P_6)\frac{\partial^5 w}{\partial x^4\partial y}\\ B_{Y2}(x,y) &= 2P_1\frac{\partial^2 w}{\partial y^2}+P_2\frac{\partial^2 w}{\partial x^2}-2P_4\frac{\partial^4 w}{\partial y^4}-(2P_5+P_6)\frac{\partial^4 w}{\partial x^2\partial y^2}-P_6\frac{\partial^4 w}{\partial x^4}\\ B_{Y3}(x,y) &= 2P_4\frac{\partial^3 w}{\partial y^3}+P_6\frac{\partial^3 w}{\partial x^2\partial y} \end{aligned} \tag{28}$$

and

C4

$$\begin{aligned} &P_1 = c_1h+c_2I,\quad P_2 = c_3h+c_2I,\quad P_3 = c_5h+c_6I,\\ &P_4 = c_7I,\quad P_5 = c_8I,\quad P_6 = c_9I \end{aligned}$$

Solving the governing equation (24) which satisfies the exact boundary conditions Eq. (27), the two-dimensional micro-plate problem will be solved.

It is clearly seen from Eqs. (24) and (25) that the present model contains all three independent material length scale parameters (l_0, l_1 and l_2), which enables the model to effectively predict the size effect. However, when two of the material length scale parameters ($l_0$and l_1) are equal to zero, the sixth-order term vanishes, then the governing equations will directly degenerate into those of the modified couple stress model (Tsiatas, 2009). Furthermore it will degenerate into the classical plate model ($(k+(4/3)\mu)I\nabla^4 w = q(x,y)$) if all of the three material length scale parameters (l_0, l_1 and l_2) are ignored (Timoshenko and Woinowsky-Krieger, 1959).

3. Static bending of simple supported size-dependent plate

Firstly, to verify the newly developed model, the static problem of a rectangular micro-plate with all edges simple supported is considered. The micro-plate is subjected to a lateral uniformly distributed load $q(x,y)$, as shown in Fig. 1.

For simple supported plate, the first, third, fourth and sixth equations in Eq. (27) are

$$\begin{aligned} &w(0,y) = 0,\quad w(a,y) = 0\\ &w_{xx}(0,y) = 0,\quad w_{xx}(a,y) = 0\\ &w(x,0) = 0,\quad w(x,b) = 0\\ &w_{yy}(x,0) = 0,\quad w_{yy}(x,b) = 0 \end{aligned} \tag{30}$$

which are the classical boundary conditions.

The higher-order boundary conditions can be obtained from the second and fifth equations in Eq. (27), that is,

$$\begin{aligned} &B_{X2}(0,y) = 0,\quad B_{X2}(a,y) = 0\\ &B_{Y2}(x,0) = 0,\quad B_{Y2}(x,b) = 0 \end{aligned} \tag{31}$$

By substituting Eq. (28) into Eq. (31), the higher-order boundary conditions are expressed as

$$\begin{aligned} &2P_1\frac{\partial^2 w(0,y)}{\partial x^2}+P_2\frac{\partial^2 w(0,y)}{\partial y^2}-2P_4\frac{\partial^4 w(0,y)}{\partial x^4}-(2P_5+P_6)\frac{\partial^4 w(0,y)}{\partial x^2\partial y^2}-P_6\frac{\partial^4 w(0,y)}{\partial y^4} = 0\\ &2P_1\frac{\partial^2 w(a,y)}{\partial x^2}+P_2\frac{\partial^2 w(a,y)}{\partial y^2}-2P_4\frac{\partial^4 w(a,y)}{\partial x^4}-(2P_5+P_6)\frac{\partial^4 w(a,y)}{\partial x^2\partial y^2}-P_6\frac{\partial^4 w(a,y)}{\partial y^4} = 0\\ &2P_1\frac{\partial^2 w(x,0)}{\partial y^2}+P_2\frac{\partial^2 w(x,0)}{\partial x^2}-2P_4\frac{\partial^4 w(x,0)}{\partial y^4}-(2P_5+P_6)\frac{\partial^4 w(x,0)}{\partial x^2\partial y^2}-P_6\frac{\partial^4 w(x,0)}{\partial x^4} = 0\\ &2P_1\frac{\partial^2 w(x,b)}{\partial y^2}+P_2\frac{\partial^2 w(x,b)}{\partial x^2}-2P_4\frac{\partial^4 w(x,b)}{\partial y^4}-(2P_5+P_6)\frac{\partial^4 w(x,b)}{\partial x^2\partial y^2}-P_6\frac{\partial^4 w(x,b)}{\partial x^4} = 0 \end{aligned} \tag{32}$$

To solve the governing equation (24) subjected to the boundary conditions in Eqs. (30) and (32), the following Fourier series is assumed for $w = w(x, y)$ in accordance with the classical case (Timoshenko and Woinowsky-Krieger, 1959) and previous work (Papargyri-Beskou and Beskos, 2009),

$$w(x,y) = \sum_{m=1}^{\infty}\sum_{n=1}^{\infty} A_{mn}\sin\left(\frac{m\pi x}{a}\right)\sin\left(\frac{n\pi y}{b}\right) \tag{33}$$

where A_{mn} are the Fourier coefficients to be determined for each m and n. It is obvious that Eq. (33) satisfies the boundary conditions in Eqs. (30) and (32). And the distributed transverse load $q(x, y)$ can also be expressed as Fourier series:

$$q(x,y) = \sum_{m=1}^{\infty}\sum_{n=1}^{\infty} Q_{mn}\sin\left(\frac{m\pi x}{a}\right)\sin\left(\frac{n\pi y}{b}\right) \tag{34}$$

For the uniformly distributed load $q(x, y) = q_0$, Q_{mn} is expressed as (Reddy, 2007b)

$$Q_{mn} = \frac{16q_0}{mn\pi^2} \quad m,n = 1,3,5,\ldots \tag{35}$$

Substituting Eqs. (33) and (34) into Eq. (24), one can deduce A_{mn} of the form

$$A_{mn} = \frac{Q_{mn}}{C_1P_1 + C_2P_2} \tag{36}$$

in which,

$$\begin{aligned} C_1 &= \left(\left(\frac{m\pi}{a}\right)^2 + \left(\frac{n\pi}{b}\right)^2\right)^3 \\ C_2 &= \left(\left(\frac{m\pi}{a}\right)^2 + \left(\frac{n\pi}{b}\right)^2\right)^2 \end{aligned} \tag{37}$$

In the following verification, without losing generality and for convenience, we assume that all the material length scale parameters in Eq. (25) are the same, i.e., $l_0 = l_1 = l_2 = Cl$, implying that the three introduced strain gradient tensors contribute equally to the size effect. In practice, the material length scale parameter Cl may be determined from fundamental mechanical tests (e.g. axial tension/compression, bending or torsion test) for specimens of different sizes. In this article, the material length scale parameter Cl is assumed to be 0.5 μm.[1] Convergence, with a tolerance of 10^{-7}, can be achieved with $m = 30$ and $n = 30$ in the calculation.

The size effect of micro-plate is illustrated below through several examples. In what follows, we keep the aspect ratio of the plate to be the same, i.e., fixing $b/h = 50$ and $a/h = 50$, and the plate Young's Modulus $E = 1.44$ GPa and Poisson's ratio $\nu = 0.3$ unless specified otherwise. To better describe the size effect, a dimensionless size scale k is introduced, which is defined as the ratio of the plate thickness to the material length scale parameter ($k = h/Cl$).

The variation of the normalized micro-plate stiffness ($abq_0/w_{\max}$) with the size scale (k) is shown in Fig. 2, where $w_{\max}$ is the plate deformation of central point ($x = a/2$, $y = b/2$). Results predicted by the present model are compared with those predicted by the modified couple stress model (Tsiatas, 2009) and the classical model (Timoshenko and Woinowsky-Krieger, 1959).

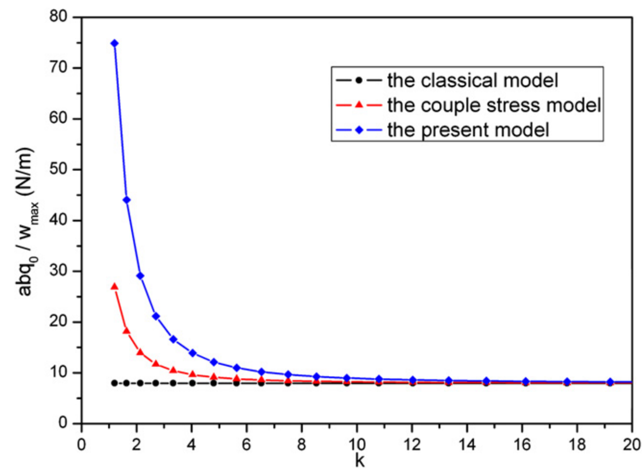

Fig. 2. Normalized stiffness with size scale.

It is seen from Fig. 2 that the normalized stiffness keeps constant for the classical model (since it has no built-in size scale), while for the present model and the modified couple stress model, the normalized stiffness increases nonlinearly as the size scale decreases. These three models show almost no difference of the normalized stiffness if the plate thickness is more than 15 times larger than the material length scale parameter; while with a smaller size scale (i.e., smaller plate dimension for the same material) the present model shows strong size effect, and that leads to a higher normalized stiffness. Although the modified couple stress model (Tsiatas, 2009) can also predict the size effect-induced increase of stiffness, the size-dependence is smaller than the present model. Specifically, when the size scale $k = 1.2$, the normalized stiffness predicted by the present model and modified couple stress model (Tsiatas, 2009) are 9.4 and 3.4 times of that by the classical model, respectively. Fundamentally speaking, the increased stiffness predicted by the present model is contributed by the three strain gradient tensors of the strain gradient elasticity theory which underpins our model, while the couple stress model (Tsiatas, 2009) introduces only the symmetric rotation gradient tensor.

The analysis indicates that for the micro-plate stiffness, the size effect may be neglected if k is larger than about 15 (and one can apply the classical model to predict the stiffness, and the present model can be reduced the classic one if the material length scale parameters are set to be zero); however, when the material length scale parameter becomes more prominent comparing with the plate thickness, in another words, when the plate is of micron dimension or smaller, the size-dependence may become strong.

4. Stability analysis of simple supported size-dependent plate

Next, we consider a rectangular micro-plate with all edges simple supported, subjecting to in-plane compressive loads $\mathbf{P} = (P_x, P_{xy}, P_y)$ and out-plane load $q(x, y)$. P_x is the load along x-axis direction, P_y is the load along y-axis direction, and P_{xy} is the in-plane shear load. According to the classical plate theory, there exists a critical buckling load $\mathbf{P}_{cr}$. The governing equation is expressed as

$$-p_1\nabla^6 w + p_2\nabla^4 w + P_x\frac{\partial^2 w}{\partial x^2} + 2P_{xy}\frac{\partial^2 w}{\partial x\partial y} + P_y\frac{\partial^2 w}{\partial y^2} = q(x,y) \tag{38}$$

For simplification, in what follows, we only consider the in-plane load component p_x, i.e., $\mathbf{P} = (p_x, 0, 0)$ and assuming $q(x, y) = 0$. Thus, Eq. (38) is rewritten as

[1] The three material length scale parameters may take different values and they can be substituted into our model independently. However, the main purpose of the present paper is to establish the theoretical framework, and the main focus is not to discuss the effect of the specific value of the length scale parameters (in part due to the lack of experiments to compare with such a variation). The easiest demonstration of the application of the framework, is therefore, assign the same value for the three length scale parameters. It is emphasized again that our model incorporates all three independent length scale parameters. The effect of the specific variation of the values of the length scale parameters will be discussed elsewhere (and hopefully better connect with experimental results where available).

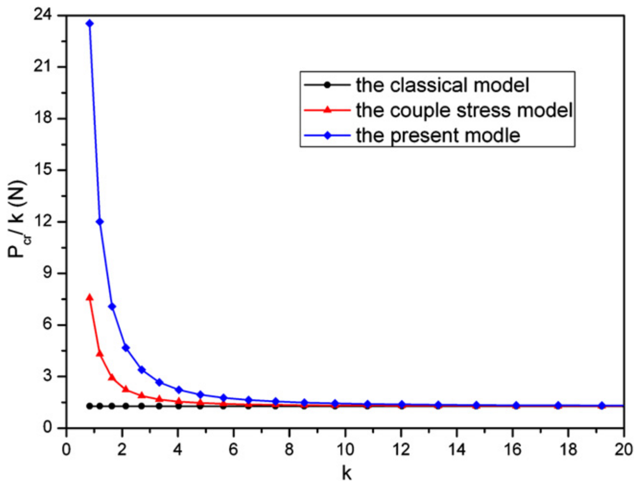

Fig. 3. Normalized critical buckling load with size scale.

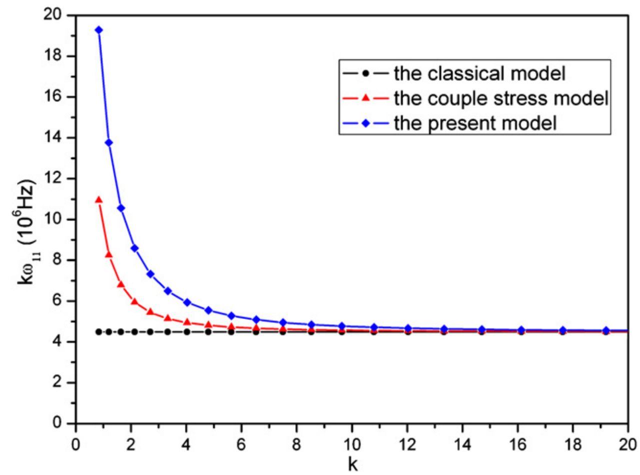

Fig. 4. Normalized natural frequency with size scale.

$$-p_1\nabla^6 w + p_2\nabla^4 w + P_x\frac{\partial^2 w}{\partial x^2} = 0 \tag{39}$$

The Fourier series solutions of Eq. (33), which satisfies with the boundary conditions in Eqs. (30) and (32), is also assumed here, and then it is substituted to Eq. (39) and is solved as

$$P_x = \frac{C_1P_1 + C_2P_2}{\left(\frac{m\pi}{a}\right)^2} \tag{40}$$

The critical buckling load P_{cr} is obtained as the minimum of P_x in Eq. (40) for appropriate positive integer values of m and n. For a square plate, in particular, the critical load P_{cr} is obtained with $m = 1$ and $n = 1$. That is,

$$P_{cr} = \left(\left(\frac{\pi}{a}\right)^2 + \left(\frac{\pi}{b}\right)^2\right)^2\left[P_1\left(1+\left(\frac{a}{b}\right)^2\right) + P_2\left(\frac{a}{\pi}\right)^2\right] \tag{41}$$

Fig. 3 shows how the normalized critical load (P_{cr}/k) varies with the size scale (k), where results of three models are presented. The parameters used are the same as those in the static problem mentioned above. In the classical theory, the critical load (P_{cr}) is proportional to the size scale (k), and thus the normalized critical load (P_{cr}/k) keeps a constant for the classical model as shown in Fig. 3. In the solutions developed from the higher-order bending theory, i.e., the present model and modified couple stress model (Tsiatas, 2009), the normalized critical load depends on the size scale of the micro-plate. The variation trend of the normalized critical load is similar to that of the normalized stiffness, and the present model predicts a larger size effect than the couple stress model does, because it introduces not only the symmetric rotation gradient tensor, but also the dilatation gradient tensor and the deviatoric stretch gradient tensor, indicating that the present model is perhaps more general and versatile than the modified couple stress model (Tsiatas, 2009).

In terms of the critical buckling load, there is almost no difference between the three models when plate thickness is more than 15 times of the material length scale parameter (Cl). While as the structure size decreases, the normalized critical load increases nonlinearly especially when the structure thickness is comparable with the material length scale parameter. The increased normalized critical load predicted by the present model indicates that the size effect is prominent as the characteristic thickness of the plate is in the order of micron or sub-micron.

5. Free vibration of simple supported size-dependent plate

Finally, we demonstrate the application of the strain gradient elasticity theory to the free flexural vibration problem of a simple supported rectangular plate. No external force is applied on the structure. Based on Eq. (24), the governing equation is written as,

$$\rho h\ddot{w} - p_1\nabla^6 w + p_2\nabla^4 w = 0 \tag{42}$$

in which w is dependent with the time scale t. Similar to the procedure of classical model (Timoshenko and Woinowsky-Krieger, 1959), the following Fourier series solutions for $w(x, y, t)$ is employed, which incorporates the spatial and temporal parts.

$$w(x,y,t) = \sum_{m=1}^{\infty}\sum_{n=1}^{\infty} B_{mn}\sin\left(\frac{m\pi x}{a}\right)\sin\left(\frac{n\pi y}{b}\right)e^{i\omega_{mn}t} \tag{43}$$

where B_{mn} is Fourier coefficient, ω_{mn} is the vibration frequency, and i is the usual imaginary number defined by $i^2 = -1$. Eq. (43) satisfies the boundary conditions in Eqs. (30) and (32) for any B_{mn}.

By substituting Eq. (43) into Eq. (42), ω_{mn}^2 is expressed as a simple form,

$$\omega_{mn}^2 = \frac{C_1P_1 + C_2P_2}{\rho h} \tag{44}$$

The positive solution of ω_{mn} determined from Eq. (44) is the natural frequency of the simple supported plate for different order number m and n. It should be noted that ω_{mn} can degenerate into the natural frequency predicted by the modified couple stress model (Tsiatas, 2009) or the classical model (Timoshenko and Woinowsky-Krieger, 1959) when two (l_0, l_1) or all (l_0, l_1, l_2) of the material length scale parameters equal to zero.

In what follows, the fundamental natural frequency for $m = 1$ and $n = 1$ is studied. The material density is set to be $\rho = 2.0 \times 10^3$ kg/m^3, and other parameters remain the same as those in Sections 3 and 4. Fig. 4 illustrates the variation of the normalized natural frequency ($k\omega_{11}$) with size scale (k). For comparison purpose, results from the other two reduced models are also given in Fig. 4. The normalized natural frequency exhibits similar size-dependent trends with that of the normalized stiffness (Section 3) and normalized critical load (Section 4). With the reduction of size scale, the normalized natural frequency always keeps constant for the classical model, while the present model predicts a nonlinearly increased normalized natural frequency. Specifically, as the size scale $k = 1.2$ and 2.7, the normalized natural frequency predicted by the present model is 3.1 and 1.6 times of that by the classical model, respectively. The size dependency of the present model is more prominent than that of the modified couple stress model (Tsiatas, 2009).

Although many researchers have developed different size-dependent models to study the dynamic problems of micro-beams (Kong et al., 2009; Ma et al., 2008; Wang et al., 2010) and micro-plate (Papargyri-Beskou and Beskos, 2008), however, to the best of authors' knowledge, the study of the size-dependent normalized natural frequency have yet not been reported in studies for micro-plate.

6. Concluding remarks

In this paper, a new size-dependent Kirchhoff micro-plate model, which contains three independent material length scale parameters, is developed. The model can reduce to the modified couple stress model and the classical model if two or all material length scale parameters are ignored. The static bending, instability and natural frequency analyses are carried out for a simple supported micro-plate to verify the new model. Numerical results reveal that the normalized stiffness, normalized critical load, and normalized natural frequency exhibit strong size-dependence. The differences of results predicted by the present model and the other two reduced models are quite large when the plate thickness is on the same order of the material length scale parameter (microns or sub-microns). These size effects are not prominent if the characteristic plate thickness is about 15 times larger than the material length scale parameter.

Note that there are several limits of the present model. First, the configuration is assumed initially stress-free; however residual stress may present in micro-devices. The incorporation of the effect of residual stress into our model will be carried out in future. Second, due to the lack of available experimental studies of the same kind, the model needs to be validated by parallel experiments in future. Moreover, different boundary constraints (other than simple supported) may be explored.

Acknowledgements

The work is supported by the National Natural Science Foundation of China (50928601 and 10572077), Specialized Research Fund for the Doctoral Program of Higher Education of China (20060422013), Natural Science Fund of Shandong Province of China (Y2007F20),WCU (World Class University) program through the National Research Foundation of Korea (R32–2008–000–20042–0), International cooperation project of Tsinghua University (20091081236), National Science Foundation (CMMI-0643726), China Scholarship Council, and Changjiang Scholar Program from Ministry of Education of China.

Appendix

The dilatation gradient tensor, γ_i ($i = 1, 2, 3$), is expressed as

$$\begin{aligned}\gamma_1 &= -z\left(\frac{\partial^3 w}{\partial x^3}+\frac{\partial^3 w}{\partial x\partial y^2}\right)\\ \gamma_2 &= -z\left(\frac{\partial^3 w}{\partial y^3}+\frac{\partial^3 w}{\partial x^2\partial y}\right)\\ \gamma_3 &= -\left(\frac{\partial^2 w}{\partial x^2}+\frac{\partial^2 w}{\partial y^2}\right)\end{aligned} \tag{45}$$

The deviatoric stretch gradient tensor, $\chi_{ij}{}^{s}$ ($i,j = 1, 2, 3$), is expressed as

$$\begin{aligned}&\chi^s_{11} = \frac{\partial^2 w}{\partial x\partial y},\quad \chi^s_{22} = -\frac{\partial^2 w}{\partial x\partial y},\quad \chi^s_{12} = \frac{1}{2}\left(\frac{\partial^2 w}{\partial y^2}-\frac{\partial^2 w}{\partial x^2}\right)\\ &\chi^s_{33} = \chi^s_{13} = \chi^s_{31} = \chi^s_{23} = \chi^s_{32} = 0\end{aligned} \tag{46}$$

The symmetric rotation gradient tensor, $\eta^{(1)}_{ijk}$ ($i, j, k = 1, 2, 3$), is expressed as

$$\begin{aligned}\eta^{(1)}_{111} &= \frac{1}{5}z\left(3\frac{\partial^3 w}{\partial x\partial y^2}-2\frac{\partial^3 w}{\partial x^3}\right)\\ \eta^{(1)}_{222} &= \frac{1}{5}z\left(3\frac{\partial^3 w}{\partial x^2\partial y}-2\frac{\partial^3 w}{\partial y^3}\right)\\ \eta^{(1)}_{333} &= \frac{1}{5}\left(\frac{\partial^2 w}{\partial x^2}+\frac{\partial^2 w}{\partial y^2}\right)\\ \eta^{(1)}_{112} &= \eta^{(1)}_{121} = \eta^{(1)}_{211} = \frac{1}{5}z\left(\frac{\partial^3 w}{\partial y^3}-4\frac{\partial^3 w}{\partial x^2\partial y}\right)\\ \eta^{(1)}_{113} &= \eta^{(1)}_{131} = \eta^{(1)}_{311} = \frac{1}{15}\left(\frac{\partial^2 w}{\partial y^2}-4\frac{\partial^2 w}{\partial x^2}\right)\\ \eta^{(1)}_{221} &= \eta^{(1)}_{212} = \eta^{(1)}_{122} = \frac{1}{5}z\left(\frac{\partial^3 w}{\partial x^3}-4\frac{\partial^3 w}{\partial x\partial y^2}\right)\\ \eta^{(1)}_{223} &= \eta^{(1)}_{232} = \eta^{(1)}_{322} = \frac{1}{15}\left(\frac{\partial^2 w}{\partial x^2}-4\frac{\partial^2 w}{\partial y^2}\right)\\ \eta^{(1)}_{331} &= \eta^{(1)}_{313} = \eta^{(1)}_{133} = \frac{1}{5}z\left(\frac{\partial^3 w}{\partial x^3}+\frac{\partial^3 w}{\partial x\partial y^2}\right)\\ \eta^{(1)}_{332} &= \eta^{(1)}_{323} = \eta^{(1)}_{233} = \frac{1}{5}z\left(\frac{\partial^3 w}{\partial y^3}+\frac{\partial^3 w}{\partial x^2\partial y}\right)\\ \eta^{(1)}_{123} &= \eta^{(1)}_{231} = \eta^{(1)}_{312} = \eta^{(1)}_{132} = \eta^{(1)}_{213} = \eta^{(1)}_{321} = \frac{1}{3}\frac{\partial^2 w}{\partial x\partial y}\end{aligned} \tag{47}$$

References

Altan, B.S., Aifantis, E.C., 1997. On some aspects in the special theory of gradient elasticity. Journal of the Mechanical Behavior of Materials 8, 231–282.
Ariman, T., 1968a. On circular micropolar plates. Archive of Applied Mechanics (Ingenieur Archiv) 37, 156–160.
Ariman, T., 1968b. Some problems in bending of micropolar plates. I & II. Bulletin de l'Academie Polonaite des Scien-ces (Applied Mechanics) 16, 295–308.
Batra, R.C., 1987. The initation and growth of, and the interation among, adiabatic shear bands in simple and dipolar materials. International Journal of Plasticity 3, 75–89.
Batra, R.C., Porfiri, M., Spinello, D., 2007. Review of modeling electrostatically actuated microelectromechanical systems. Smart Materials and Structures 16, R23–R31.
Chasiotis, I., Knauss, W.G., 2003. The mechanical strength of polysilicon films: part 2. Size effects associated with elliptical and circular perforations. Journal of the Mechanics and Physics of Solids 51, 1551–1572.
Ellis, R.W., Smith, C.W., 1967. A thin-plate analysis and experimental evaluation of couple-stress effects. Experimental Mechanics 7, 372–380.
Exadaktylos, G.E., Vardoulakis, I., 2001. Microstructure in linear elasticity and scale effects: a reconsideration of basic rock mechanics and rock fracture mechanics. Tectonophysics 335, 81–109.
Fleck, N.A., Hutchinson, J.W., 1993. A phenomenological theory for strain gradient effects in plasticity. Journal of the Mechanics and Physics of Solids 41, 1825–1857.
Fleck, N.A., Muller, G.M., Ashby, M.F., Hutchinson, J.W., 1994. Strain gradient plasticity – theory and experiment. Acta Metallurgica et Materialia 42, 475–487.
Hoffman, O., 1964. On bending of thin elastic plates in the presence of couple stresses. Journal of Applied Mechanics – ASME 31, 706–707.
Kong, S.L., Zhou, S.J., Nie, Z.F., Wang, K., 2009. Static and dynamic analysis of micro beams based on strain gradient elasticity theory. International Journal of Engineering Science 47, 487–498.
Lam, D.C.C., Chong, A.C.M., 1999. Indentation model and strain gradient plasticity law for glassy polymers. Journal of Materials Research 14, 3784–3788.
Lam, D.C.C., Yang, F., Chong, A.C.M., Wang, J., Tong, P., 2003. Experiments and theory in strain gradient elasticity. Journal of the Mechanics and Physics of Solids 51, 1477–1508.
Lazopoulos, K.A., 2004. On the gradient strain elasticity theory of plates. European Journal of Mechanics – A/Solids 23, 843–852.
Lazopoulos, K.A., 2009. On bending of strain gradient elastic micro-plates. Mechanics Research Communications 36, 777–783.

Ma, H.M., Gao, X.L., Reddy, J.N., 2008. A microstructure-dependent Timoshenko beam model based on a modified couple stress theory. Journal of the Mechanics and Physics of Solids 56, 3379–3391.
McFarland, A.W., Colton, J.S., 2005. Role of material microstructure in plate stiffness with relevance to microcantilever sensors. Journal of Micromechanics and Microengineering 15, 1060–1067.
Mindlin, R.D., 1964. Micro-structure in linear elasticity. Archive for Rational Mechanics and Analysis 16, 51–78.
Mindlin, R.D., 1965. Second gradient of strain and surface-tention in linear elasticity. International Journal of Solids and Structures 1, 417–438.
Nix, W.D., 1989. Mechanical-properties of thin-films. Metallurgical Transactions A – Physical Metallurgy and Materials Science 20, 2217–2245.
Papargyri-Beskou, S., Beskos, D.E., 2008. Static, stability and dynamic analysis of gradient elastic flexural Kirchhoff plates. Archive of Applied Mechanics (Ingenieur Archiv) 78, 625–635.
Papargyri-Beskou, S., Beskos, D.E., 2009. Stability analysis of gradient elastic circular cylindrical thin shells. International Journal of Engineering Science 47, 1379–1385.
Papargyri-Beskou, S., Tsepoura, K.G., Polyzos, D., Beskos, D.E., 2003. Bending and stability analysis of gradient elastic beams. International Journal of Solids and Structures 40, 385–400.
Papargyri-Beskou, S., Giannakopoulos, A.E., Beskos, D.E., 2010. Variational analysis of gradient elastic flexural plates under static loading. International Journal of Solids and Structures 47, 2755–2766.
Poole, W.J., Ashby, M.F., Fleck, N.A., 1996. Micro-hardness of annealed and work-hardened copper polycrystals. Scripta Materialia 34, 559–564.
Reddy, J.N., 2007a. Nonlocal theories for bending, buckling and vibration of beams. International Journal of Engineering Science 45, 288–307.
Reddy, J.N., 2007b. Theory and Analysis of Elastic Plates and Shells, second ed. Taylor & Francis, Philadelphia, PA.
Shu, J.Y., Fleck, N.A., 1998. The prediction of a size effect in micro-indentation. International Journal of Solids and Structures 35, 1363–1383.
Timoshenko, S., Woinowsky-Krieger, S., 1959. Theory of Plates and Shells, second ed. McGraw-Hill Book Company, New York.
Tsiatas, G.C., 2009. A new Kirchhoff plate model based on a modified couple stress theory. International Journal of Solids and Structures 46, 2757–2764.
Vardoulakis, I., Exadaktylos, G., Kourkoulis, S.K., 1998. Bending of marble with intrinsic length scales: a gradient theory with surface energy and size effects. Journal de Physique IV 8, 399–406.
Vardoulakis, I., Sulem, J., 1995. Bifurcation Analysis in Geomechanics. Chapman and Hall, London.
Vavva, M.G., Protopappas, V.C., Gergidis, L.N., Charalambopoulos, A., Fotiadis, D.I., Polyzos, D., 2009. Velocity dispersion of guided waves propagating in a free gradient elastic plate: application to cortical bone. Journal of the Acoustical Society of America 125, 3414–3427.
Wang, B., Zhou, S., Zhao, J., 2010. A micro scale Timoshenko beam model based on strain gradient elasticity theory. European Journal of Mechanics – A/Solids 29, 591–599.
Yang, F., Chong, A.C.M., Lam, D.C.C., Tong, P., 2002. Couple stress based strain gradient theory for elasticity. International Journal of Solids and Structures 39, 2731–2743.